Supporting Information

Core-shell silicon nanowire solar cells

M M Adachi [1 2], *M P Anantram* [3], *K S Karim* [1 2]

[1]Department of Electrical and Computer Engineering; and [2]Waterloo Institute for Nanotechnology, University of Waterloo, Waterloo, ON, N2G 3G1, Canada

[3]Department of Electrical Engineering, University of Washington, Seattle, WA, USA

Nanowire sidewall coverage.

Figure S1 shows a magnified SEM image of the Si nanowire array (l~800nm) after n+ deposition with areas circled at the nanowire base where n+ film coverage is either thin or absent. Low side-wall coverage is due to shadowing effects during deposition caused by the high density of nanowires or possibly poor adhesion to the ZnO:Al shell. Furthermore, the growth conditions were mass transport limited resulting in faster growth near the nanowire tip and slower growth at the nanowire base. Conformal growth can be improved by using a low plasma power density and higher gas source concentration 1.

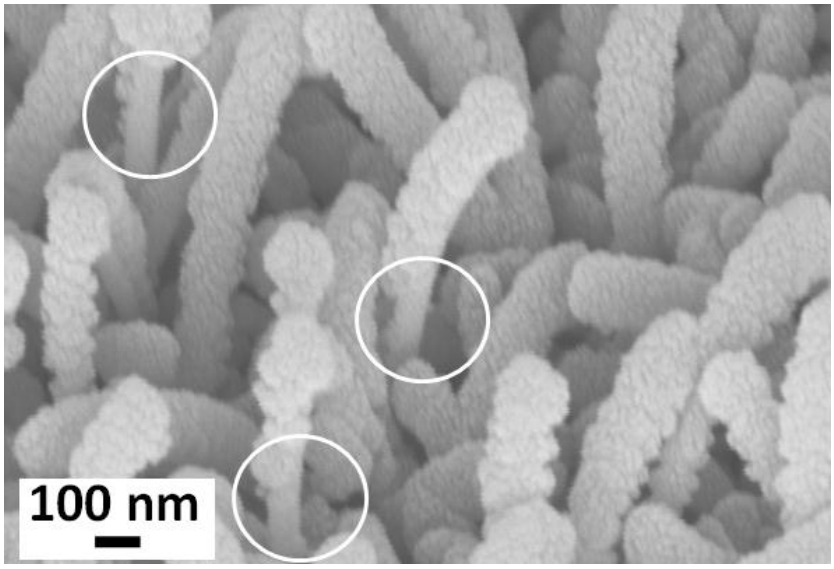

Figure S1. Nanowire sidewall coverage. SEM (45° tilt) of the Si nanowire array (l~800nm) after n+ layer deposition. The circles indicate regions near the base of nanowires where n+ Si shell coverage is poor.

Amorphous Si nanowire shell solar cells with different shell thicknesses.

The total reflectance of amorphous Si nanowire shell solar cells with three different total diameters (without top ZnO:Al contact) d of 320 nm, 360 nm, and 590 nm are shown in Figure S2a. The nanowire device with a d = 360 nm is the same device shown in Figure 3. The two smaller diameter arrays, d = 320 and 360 nm, exhibit similarly low total reflectance of ≤5% over the wavelength range λ = 400 to 650 nm. However, the reflectance of the largest diameter array d = 590 nm is slightly higher, at 8% over the same wavelength range. Nonetheless, all core-shell nanowire devices exhibit significantly lower total reflectance than the planar control device shown in Figure 3a.

The external quantum efficiency (EQE) of the three amorphous Si nanowire shell solar cells with differing diameters is shown in Figure S2b. The device with an average diameter of d

= 360 nm exhibits the highest broadband EQE. The smaller diameter device d = 320 nm shows lower EQE than the larger diameter devices, particularly at longer wavelengths (λ = 450 to 750 nm), due to insufficient optical absorption in the thin intrinsic amorphous Si shell. Conversely, the largest diameter device d = 590 nm exhibits high EQE at long wavelengths but low EQE at short wavelengths (λ=300 to 550 nm) due to absorption losses in the p+ layer. That is, the p+ deposition time was tailored for sufficiently covering the nanowire sidewall of the device with a diameter of d = 360 nm but the same deposition conditions were used for all three devices with different diameters. The lower aspect ratio of the large diameter nanowires therefore resulted in thicker p+ Si shell on the nanowire top surface. Consequently, tailoring of the p+ Si shell deposition time is necessary for different Si nanowire diameters.

The J-V curves for the amorphous Si nanowire shell solar cells under AM1.5 global illumination are shown in Figure S2c. The device characteristics are Voc = 0.794V, Jsc = 11.86 mA/cm2, fill factor = 50.0%, η = 4.70% for the smallest diameter device (d = 320 nm), and Voc = 0.855V, Jsc = 13.0 mA/cm2, fill factor = 47.9%, η = 5.33% for the largest diameter device (d = 590 nm). The device with a diameter of d=360 nm has a Voc = 0.830V, Jsc = 13.9 mA/cm2, fill factor = 52.4%, η = 6.0%. The high overall conversion efficiency of this device can be attributed to low optical reflectance (Figure S2a) and the p+ shell thickness being tailored for this diameter, leading to high fill factor.

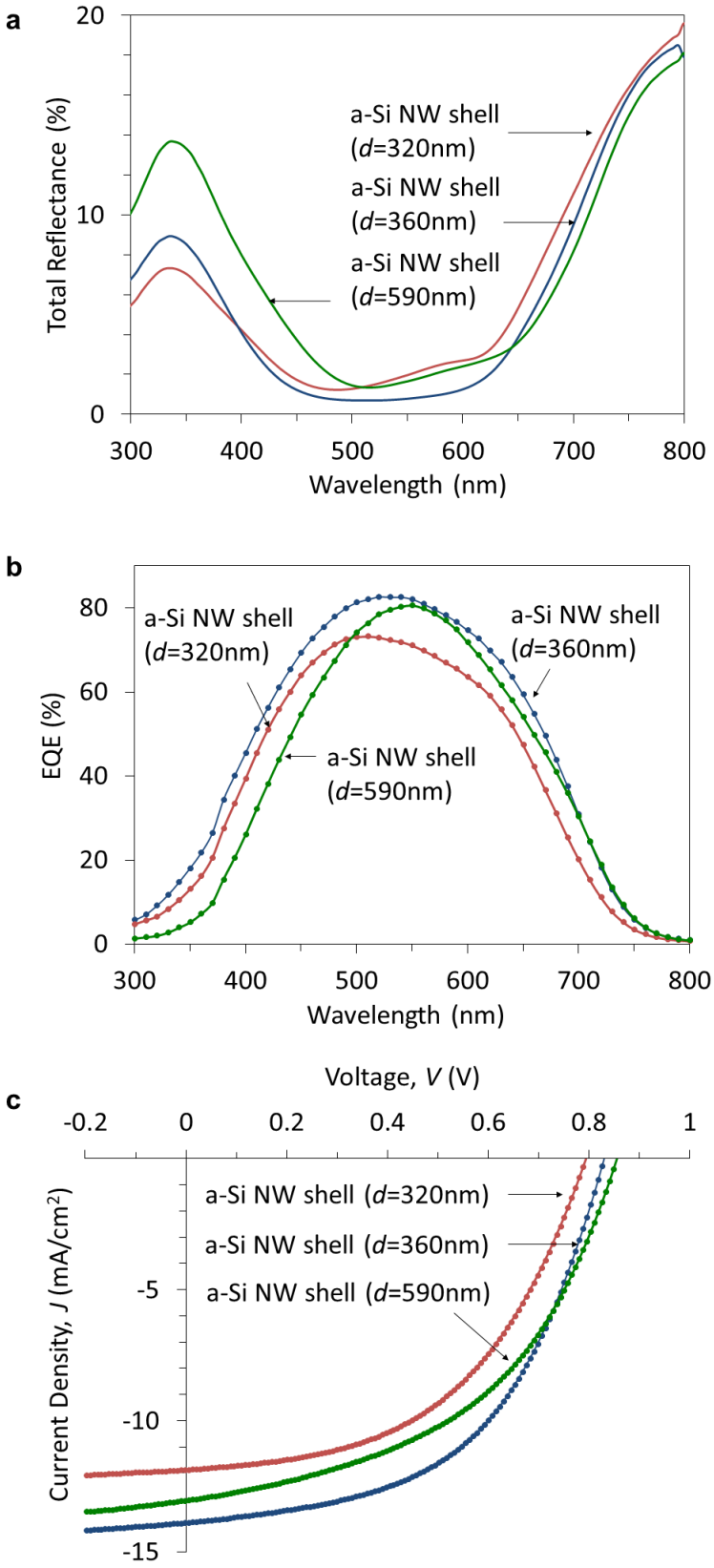
a
Total Reflectance (%)
Wavelength (nm)
a-Si NW shell (d=320nm)
a-Si NW shell (d=360nm)
a-Si NW shell (d=590nm)
b
EQE (%)
Wavelength (nm)
a-Si NW shell (d=320nm)
a-Si NW shell (d=360nm)
a-Si NW shell (d=590nm)
c
Voltage, V (V)
Current Density, J (mA/cm²)
a-Si NW shell (d=320nm)
a-Si NW shell (d=360nm)
a-Si NW shell (d=590nm)

Figure S2. Performance of amorphous Si nanowire shell solar cells with varying diameters. (a) Total (specular and diffuse) reflectance of nanocrystalline Si (nc-Si) nanowire (NW) shell solar cells with an average total NW diameter (without top ZnO:Al contact) d of 320 nm, 360 nm, and 590 nm. (b) external quantum efficiency (EQE) spectra of the amorphous Si nanowire shell solar cells. (C) J-V curves under AM 1.5 global illumination (100mW/cm2) of the amorphous Si nanowire shell solar cells.

Nanocrystalline Si nanowire shell solar cells.

An SEM image of a highly dense array of Si nanowires grown on Al-coated glass is shown in Figure S3a. The average length of the nanowires is 800 nm, and the average diameter is 30 nm. The nanowires are again covered with a thin layer of ZnO:Al to prevent counter-doping of the n+ layer by the Al back contact. The ZnO:Al covered nanowires have an average total diameter of about 55 nm, and are shown in Figure S3b. Due to stress and non-conformal deposition of the ZnO:Al film some nanowires are slightly bent. The nanowire array with n+ shell is shown in Figure S3c, and the final device after n-i-p and top ZnO:Al deposition is shown in Figure S3d. The radial thickness of the n+ shell is approximately 40 nm. The nanocrystalline Si intrinsic shell was deposited under high-pressure (7 Torr) and high-power (0.37W/cm2) conditions, leading to tapered sidewalls. The final core-shell nanowire device with ZnO:Al top contact consists of a large rounded top with an average diameter of about 560 nm and narrow base diameter of approximately 135 nm.

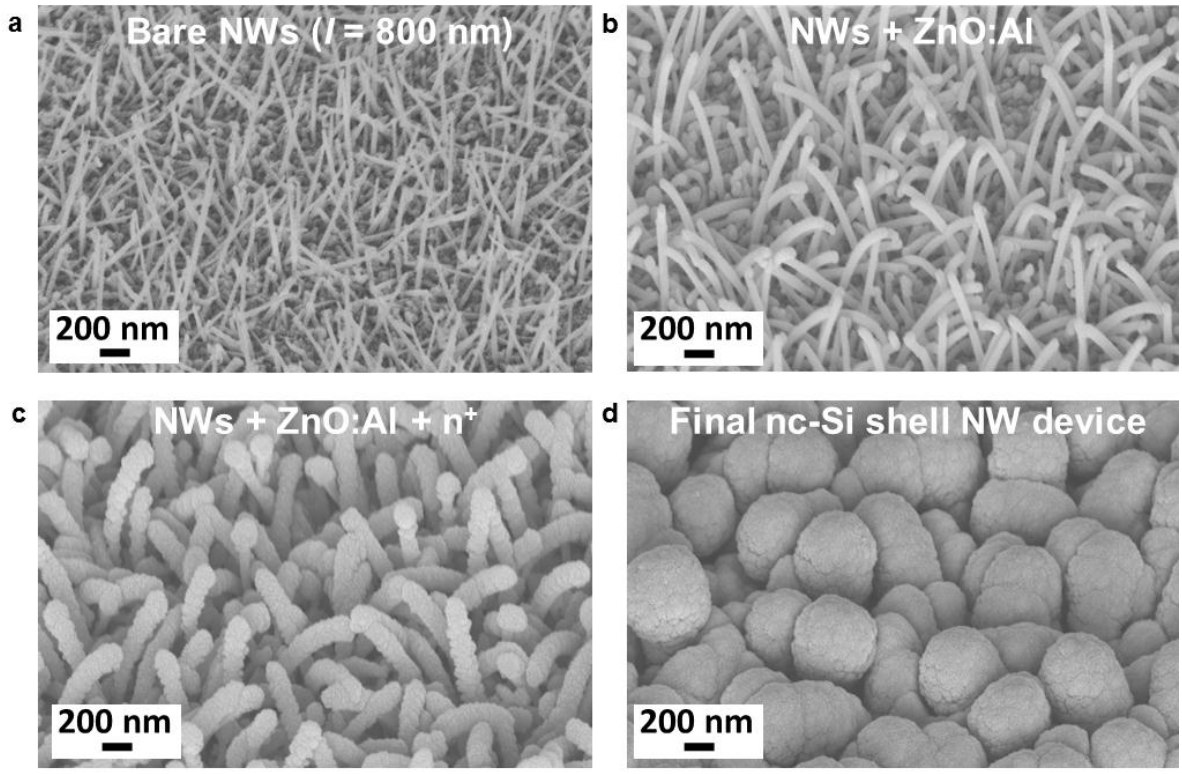

Figure S3. Nanocrystalline Si nanowire shell solar cells at different stages of fabrication. SEM (45° tilt) images of bare Si nanowires (NWs) (a), nanowires with ZnO:Al coating (b), nanowires coated with ZnO:Al and n+ shell (c). The average nanowire length is 800 nm. (d) SEM (45° tilt) image of the final fabricated n-i-p radial nanowire solar cell with nanocrystalline Si (nc-Si) intrinsic shell (without gridlines).

References:

1. Tsai, C.C.; Knights, J.C.; Chang, G.; Wacker, B. J. Appl. Phys.1986, 59, 2998-3001.